

Electronic Supplementary Information

A versatile quinoxaline derivative serves as a colorimetric sensor for strongly acidic pH

Riya Bag,^a Yeasin Sikdar,^a Sutapa Sahu,^a Dilip K. Maiti,^a Antonio Frontera,^b Antonio Bauzá,^b Michael G. B. Drew,^c and Sanchita Goswami^{*a}

^aDepartment of Chemistry, University of Calcutta, 92, A.P.C. Road, Kolkata, India.

E-mail: sgchem@caluniv.ac.in

^bDepartament de Química, Universitat de les Illes Balears, Crta. de Valldemossa km 7.5, 07122 Palma de Mallorca, Balears, Spain

^cDepartment of Chemistry, University of Reading, Whiteknights, Reading RG6 6AD, UK

Contents of the Supporting Information

	Page No.
Fig. S1 ¹ H NMR spectrum of HQphy in <i>d</i> ₆ -DMSO.	S5
Fig. S2 ¹³ C NMR spectrum of HQphy in <i>d</i> ₆ -DMSO.	S6
Fig. S3 ¹ H NMR Spectrum of HQphy in absence (below) and in presence (above) of perchloric acid in CDCl ₃ .	S7
Fig. S4 ESI-MS Spectrum of HQphy .	S8
Fig. S5 ESI-MS Spectrum of [H ₂ Qphy]ClO ₄ ·H ₂ O.	S9
Fig. S6 FT-IR Spectrum of HQphy (1), [HQphy][FeCl ₄]·H ₂ O (2), [H ₂ Qphy]ClO ₄ ·H ₂ O (3) and [H ₂ Qphy] ₂ S·4H ₂ O (4).	S10
Fig. S7 Experimental (Red) and calculated (black) Powder X-ray diffraction spectrum of (A) HQphy , (B) [HQphy][FeCl ₄]·H ₂ O, (C) [H ₂ Qphy]ClO ₄ ·H ₂ O and (D) [H ₂ Qphy] ₂ S·4H ₂ O to determine the phase purity.	S11
Fig. S8 Powder X-ray diffraction spectrum of complex 3 after transformation from 1 .	S12
Fig. S9 UV-Vis absorption spectra of HQphy (10 μM) upon addition of 10 μM metal ions (perchlorate or chloride salts of Na ⁺ , K ⁺ , Ca ²⁺ , Mg ²⁺ , Hg ²⁺ , Ni ²⁺ , Fe ³⁺ , Cu ²⁺ , Co ²⁺ , Cd ²⁺ , Zn ²⁺ , Fe ²⁺ , Mn ²⁺ , Cr ³⁺ and Al ³⁺) in acetonitrile medium.	S12

Fig. S10 UV–Vis absorption spectra of **HQphy** (10 μM) upon addition of 50 μM different anions (tetrabutyl ammonium salts of F^- , OAc^- , Cl^- , Br^- , I^- , HSO_4^- , NO_3^- , SCN^- , ClO_4^- and PF_6^-) in acetonitrile medium. S13

Fig. S11 UV–Vis absorption spectra of probe **HQphy** in presence of Fe^{3+} , water and at pH 0.48. S13

Fig. S12 X–band EPR spectra of solid $[\text{HQphy}][\text{FeCl}_4]\cdot\text{H}_2\text{O}$ (**2**) at room temperature (Frequency– 9.46494 GHz). S14

Fig. S13 Molecular structures of Compound **4** ($[\text{H}_2\text{Qphy}]_2\text{S}\cdot 4\text{H}_2\text{O}$) in ball and stick representation. Only H–bonds between protonated nitrogen (N4) and lattice water are shown as dotted turquoise bonds. The cation is disordered over a pseudo mirror plane through C7–H7, only the major component is shown. Color code: C = green; N = blue; O = red; S = maroon; H= yellow. S14

Supramolecular Structures of 1–4 S15

Fig. S14 (**HQphy**) (A) Infinite 1–D chain mediated by N–H \cdots N hydrogen bonding interactions and π – π interactions between parallel quinoxaline and phenyl moieties (two opposite intercalated nearly parallel tapes are shown in green and orange colors). (B) Enlarged view of π – π and N–H \cdots N hydrogen bonding interactions with partial atom numbering. The centroid X and Y are formed by atom groups C8 C9 N3 C10 C15 N4 and C1–C6 inclusive respectively. The centroid–centroid distance is 3.7032(14) Å. Turquoise bond represents the H–bond. Symmetry elements #1 ($-1+x, +y, +z$); #2 ($1/2+x, 3/2-y, -z$). S17

Fig. S15 ($[\text{H}_2\text{Qphy}][\text{FeCl}_4]\cdot\text{H}_2\text{O}$) (A) 3–D supramolecular association of protonated ligand with lattice water and tetrahedral FeCl_4^- ion (shown in polyhedra) (B) Local environment around tetrahedral FeCl_4^- ion stabilized by aromatic C–H \cdots Cl, N–H \cdots Cl, N–H \cdots O, O–H \cdots N interactions and bifurcated π – π stacking between phenyl group and quinoxaline moiety. The three centroids X, Y, Z, are formed from rings containing atoms C8 C9 N3 C10 C15 N4, C1–C6 inclusive, C10–C15 inclusive respectively. Symmetry transformations are #1 ($1+x, -1+y, z$); #2 ($-1+x, y, z$); #3 ($x, 2-y, 1/2+z$); #4 ($x, 1-y, 1/2+z$). The marked centroid–centroid distances are 3.689(2) Å [X–Y#2], 3.765(3) Å [Y#2–Z], 3.869(3) Å [Y–Z#1]. H–bonds are shown as dotted turquoise bonds. S18

Fig. S16 $[\text{H}_2\text{Qphy}]\text{ClO}_4\cdot\text{H}_2\text{O}$ (A) Each of the octameric water–perchlorate clusters S19

encapsulated by two ligand is stacked over one another through π - π stacking along the *b* axis. Along the *c* axis, this octameric entity interacts with another through C-H \cdots N interactions to form 2-D sheet. Each of the 2-D sheets are stitched over one another through Cl-O \cdots π interaction to form 3-D supramolecular interaction. (B) Enlarged view of water-perchlorate association via hydrogen bonding and π - π stacking. The centroids X, Y are formed from rings containing atoms C8 C9 N3 C10 C15 N4, and C1-C6 inclusive. The marked centroid-centroid distance is 3.618(2) Å. (C) Chair-like octameric association of [(H₂O)₂(ClO₄)₂]²⁻ anion water cluster. H-bonds are shown as dotted turquoise bonds. Symmetry code for the equivalent atoms, #1 (-x, 1/2+y, 1/2-z); #2 (-x, 1-y, 1-z); #3 (+x, 1/2-y, 1/2+z); #4 (x, -1+y, z); #5 (-x, 2-y, 1-z).

Fig. S17 ([H₂Qphy]₂S \cdot 4H₂O) (A) Infinite 3-D sheet like structure formed by various hydrogen bonding interactions N-H \cdots O, N-H \cdots S, O-H \cdots O, O-H \cdots S (details in Table S6) and π - π stacking seen through *a* axis. (B) Encapsulation of hydrophobic π - π interaction mediated by cationic H₂Qphy within the hydrogen bonded 2-D layer of [S(H₂O)₆]²⁻. (C) Enlarged view of π - π interaction with the centroids X and Z are formed by atom groups N1 C6 C1 N3X C9X C2X and C1-C6 inclusive respectively. The centroid-centroid distance is 3.530(3) Å. (D) Enlarged view of hydrogen bonded lattice water molecule to form 1-D water chain, which forms head-on hydrogen bonding via sulfide ion to another 1-D chain to form 2-D sulfide-water cluster. H-bonds are shown as dotted turquoise bonds. The symmetry elements #1 (+x, -1+y, +z); #2 (1-x, -1+y, 3/2-z); #3 (1-x, +y, 3/2-z); #4 (1-x, 1+y, 3/2-z); #5 (1-x, 2+y, 3/2-z); #6 (+x, 2+y, +z); #7 (+x, 1+y, +z); #8 (1-x, 1-y, 1-z); #9 (1-x, -y, 1-z); #10 (+x, -y, -1/2+z); #11 (+x, 1-y, -1/2+z); #12 (+x, 2-y, -1/2+z); #13 (+x, 3-y, -1/2+z); #14 (1-x, 3-y, 1-z); #15 (1-x, 2-y, 1-z).

Fig. S18 Frontier molecular orbitals involved in three observable UV-Vis absorption bands of the probe.

Fig. S19 (A) UV-Vis absorption spectra and (B) Visual color change of HQphy (10 μ M) from yellow to red upon addition of 0.1 mM of different acetic acids (where, Aa = acetic acid).

Table S1 Strongly acidic pH sensing probes found in literature.

Table S2 Crystal Data and refinement details for complexes 1-4.

Table S3 Some important comparable metric parameters (distances, Å, angles (°)) in HQphy , [H₂Qphy][FeCl₄·H₂O] , [H₂Qphy]ClO₄·H₂O and [H₂Qphy]₂S·4H₂O .	S26
Table S4 Hydrogen bonds parameters in complex 1–4 , (distances, Å, angles, (°)).	S27
Table S5 Various π – π stacking interactions observed in Complexes 1–4 .	S28
Table S6 Selected parameters for the vertical excitation (UV–Vis absorptions) of HQphy , electronic excitation energies (eV) and oscillator strengths (<i>f</i>), configurations of the low–lying excited states of HQphy ; calculation of the S ₀ –S _n energy gaps based on optimized ground–state geometries (UV–Vis absorption, acetonitrile used as solvent). For each electronic transition, only those contributions higher than 20% are given.	S29
Table S7 Selected parameters for the vertical excitation (UV–Vis absorptions) of protonated compound (H₂Qphy⁺), electronic excitation energy (eV) and oscillator strength (<i>f</i>), configurations of the lowest–lying excited state; calculation of the S ₀ –S _n energy gaps based on optimized ground–state geometries (UV–Vis absorption, in water solvent).	S30

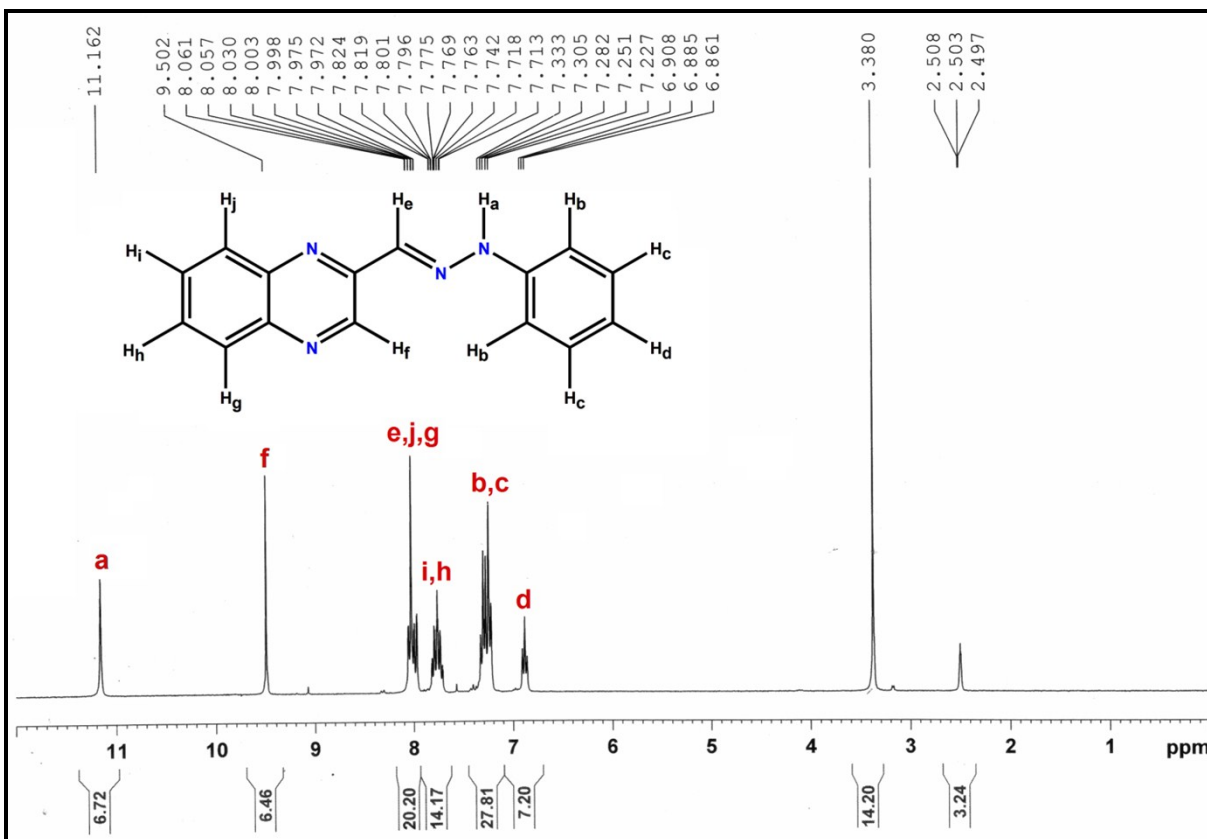


Fig. S1 ¹H NMR spectrum of HQphy in *d*₆-DMSO.

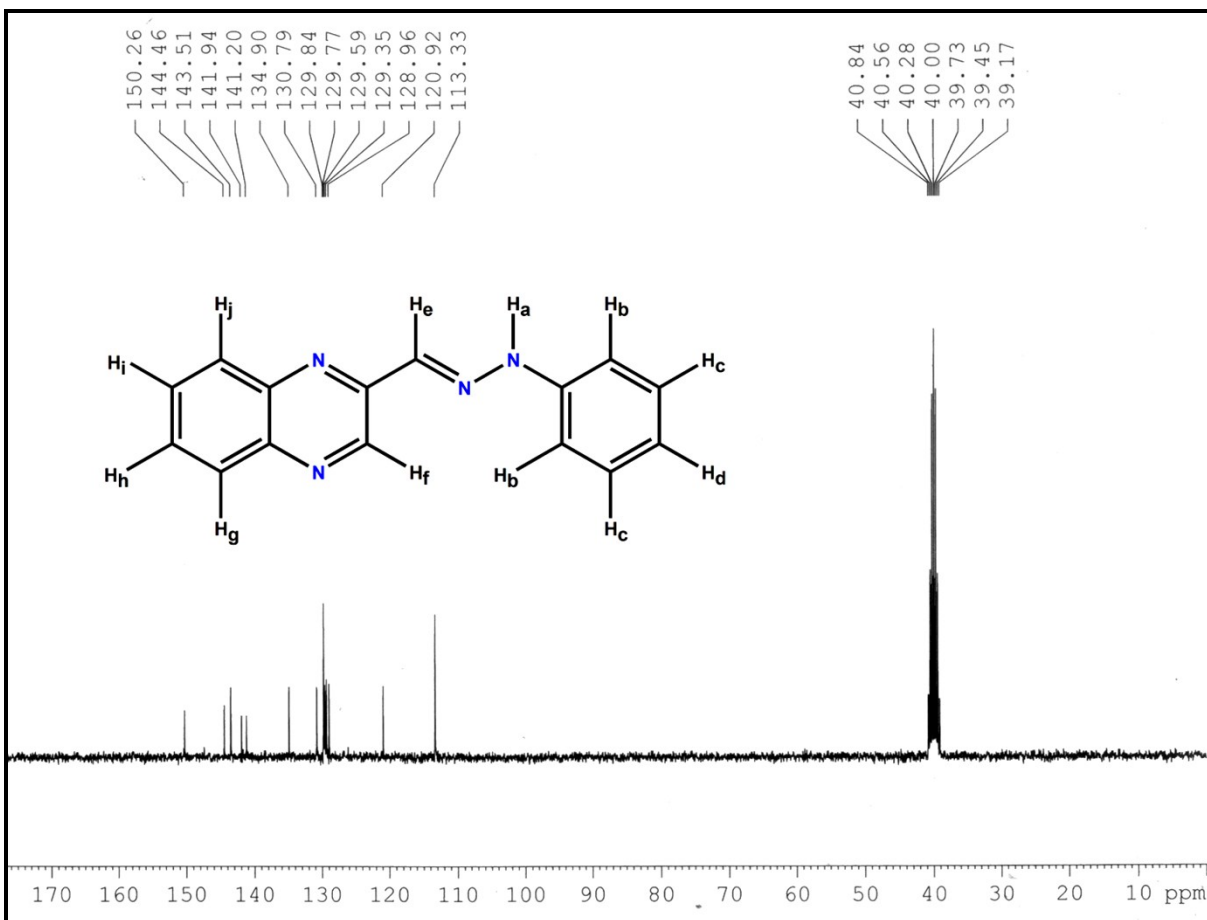


Fig. S2 ^{13}C NMR spectrum of **HQphy** in d_6 -DMSO.

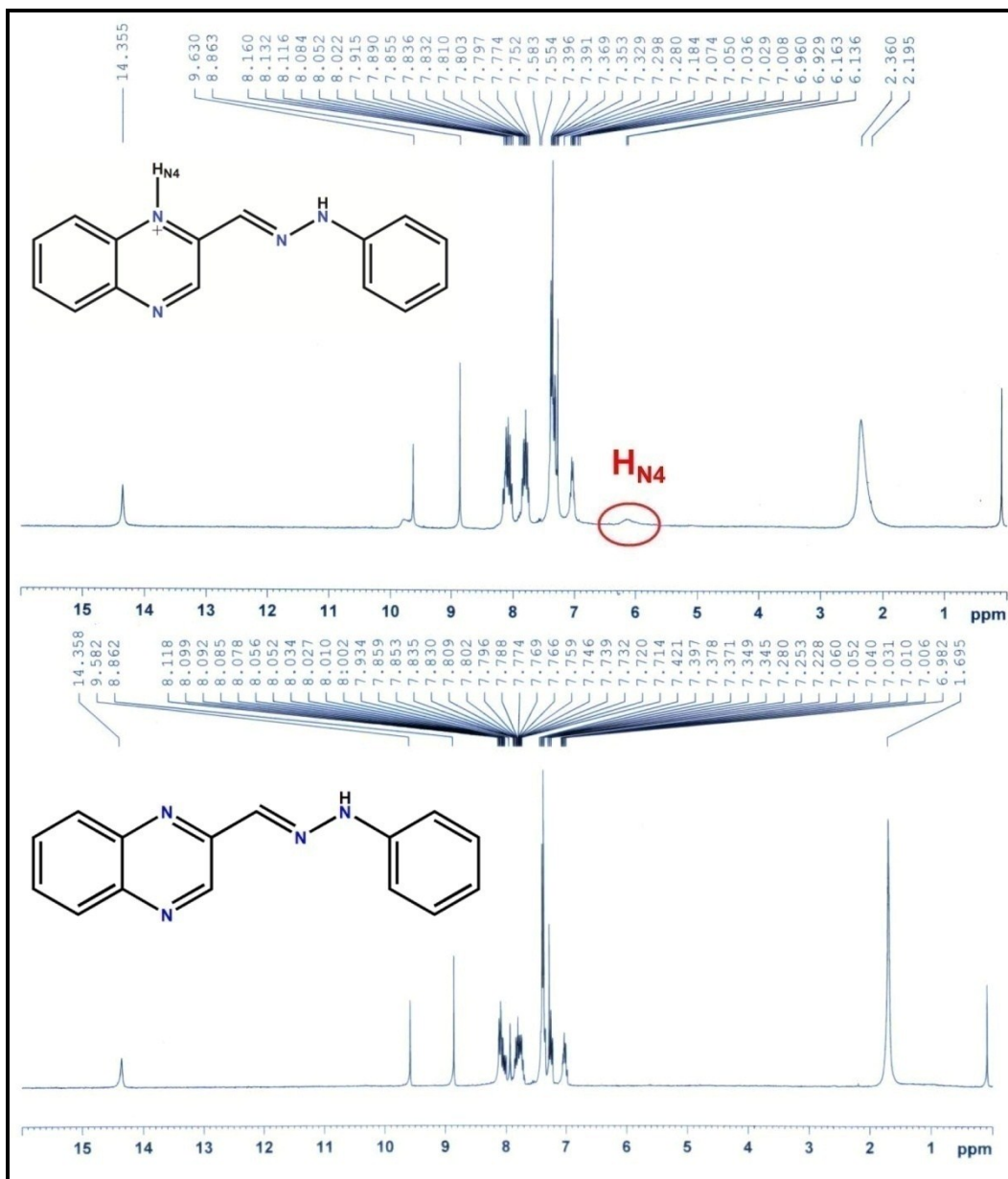


Fig. S3 ¹H NMR Spectrum of **HQphy** in absence (below) and in presence (above) of perchloric acid in CDCl₃.

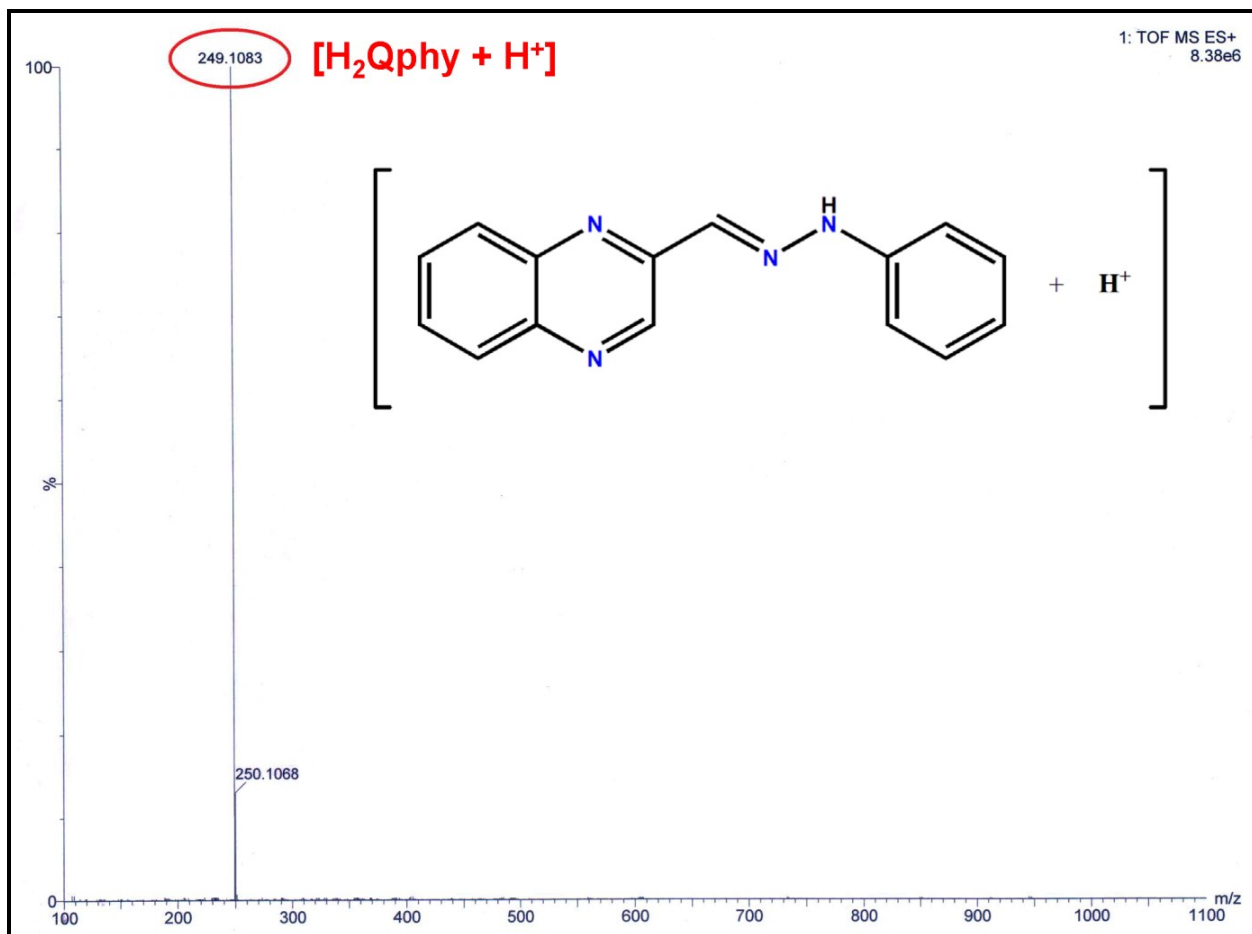


Fig. S4 ESI-MS Spectrum of **HQphy**.

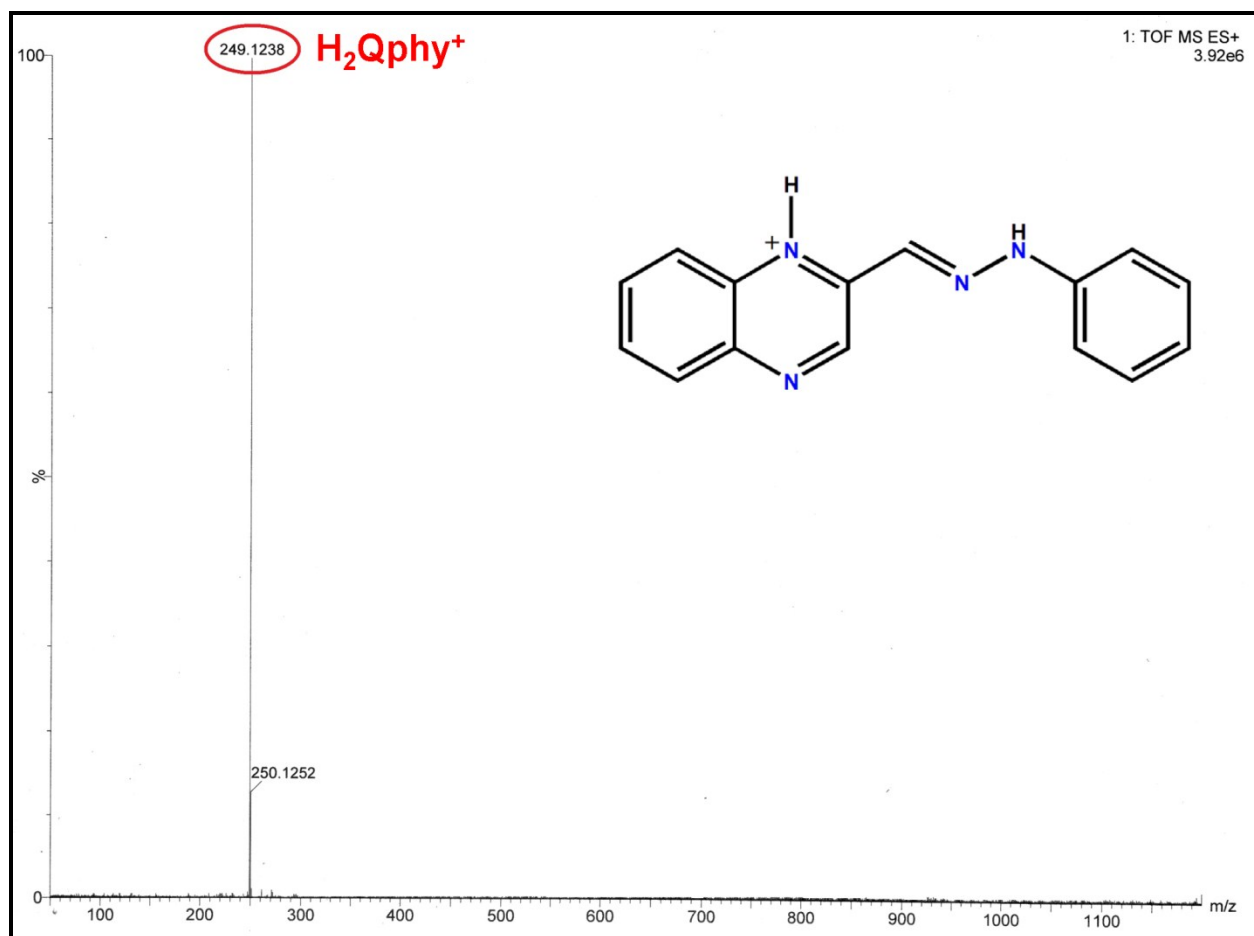


Fig. S5 ESI-MS Spectrum of $[H_2Qphy]ClO_4 \cdot H_2O$.

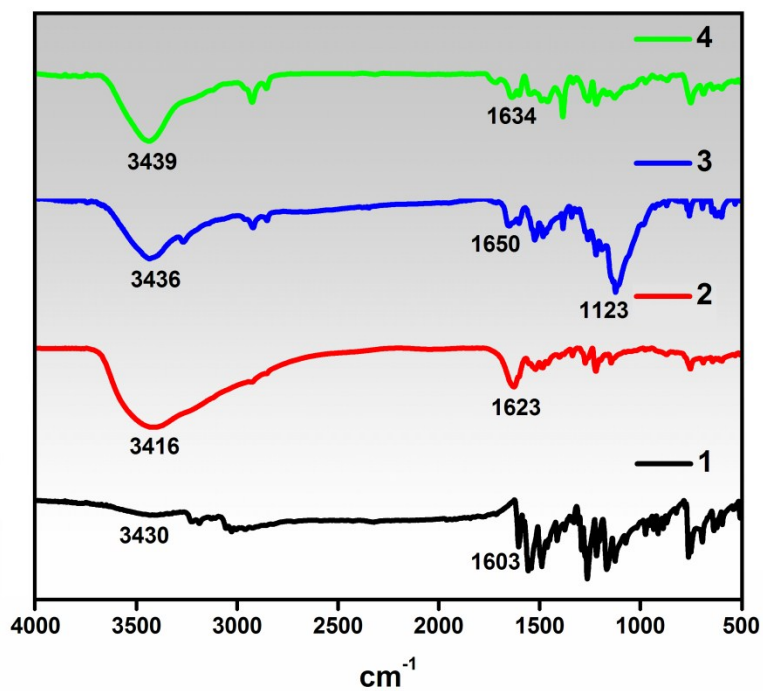


Fig. S6 FT-IR Spectrum of **HQphy** (1), **[HQphy][FeCl₄]·H₂O** (2), **[H₂Qphy]ClO₄·H₂O** (3) and **[H₂Qphy]₂S·4H₂O** (4).

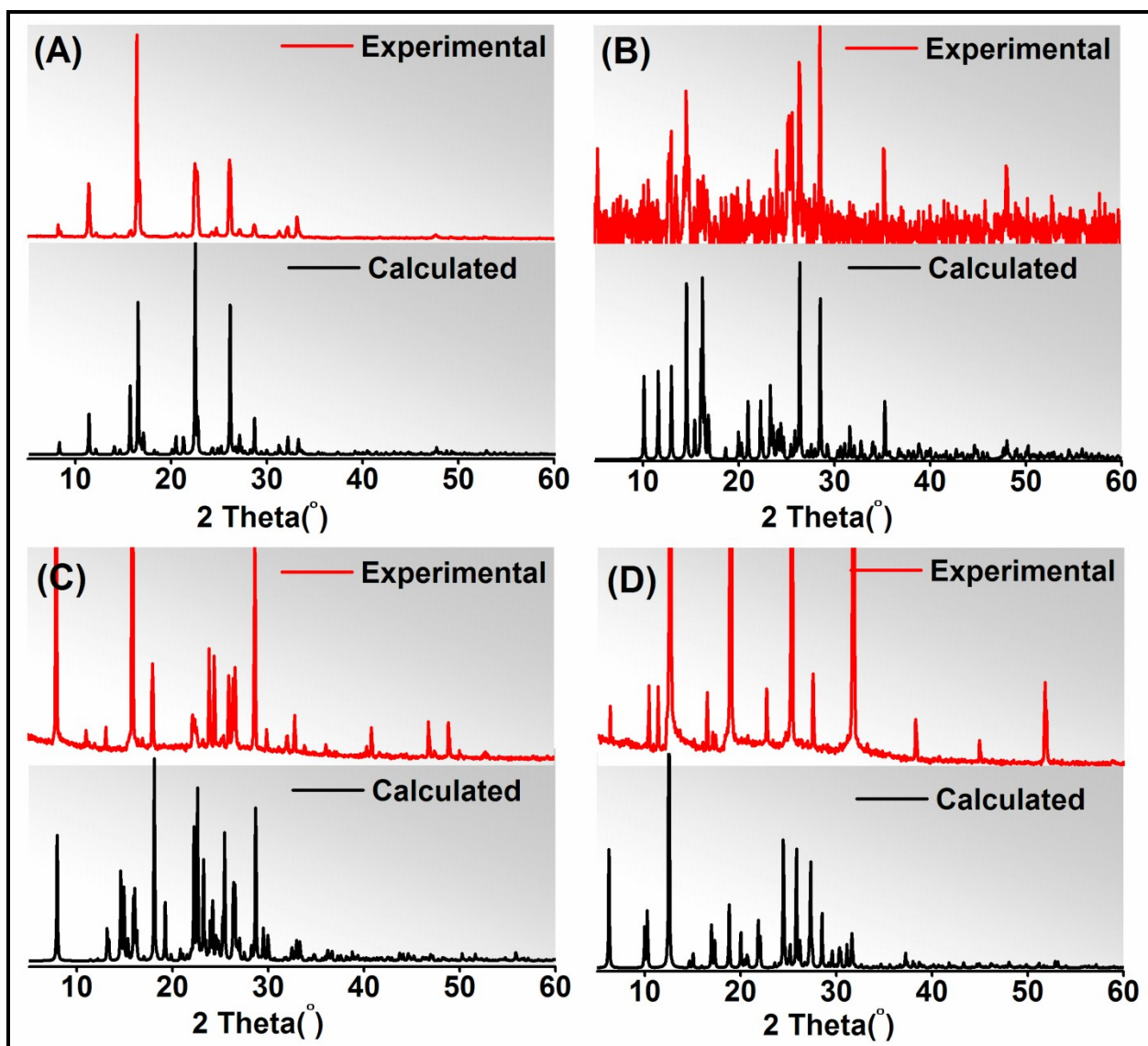


Fig. S7 Experimental (Red) and calculated (black) Powder X-ray diffraction spectrum of (A) HQphy, (B) [HQphy][FeCl₄] \cdot H₂O, (C) [H₂Qphy]ClO₄ \cdot H₂O and (D) [H₂Qphy]₂S \cdot 4H₂O to determine the phase purity.

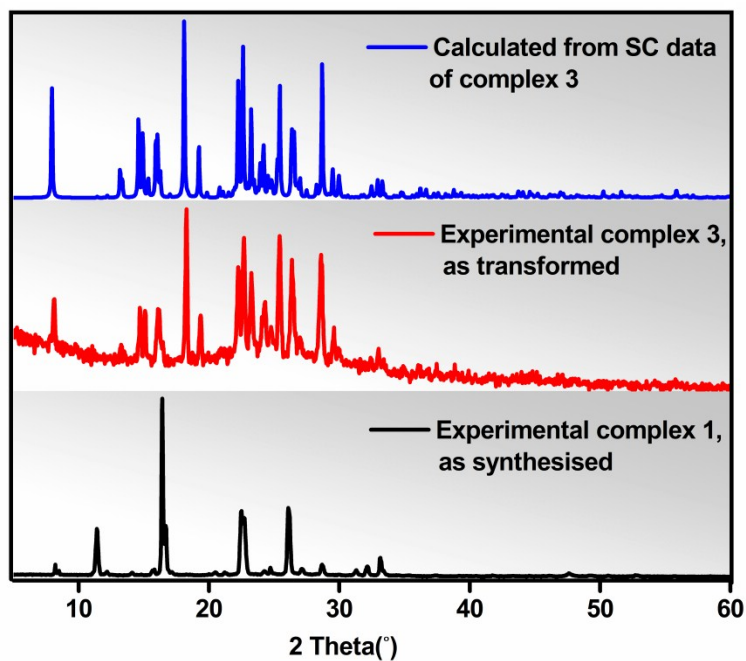


Fig. S8 Powder X-ray diffraction spectrum of complex **3** after transformation from **1**.

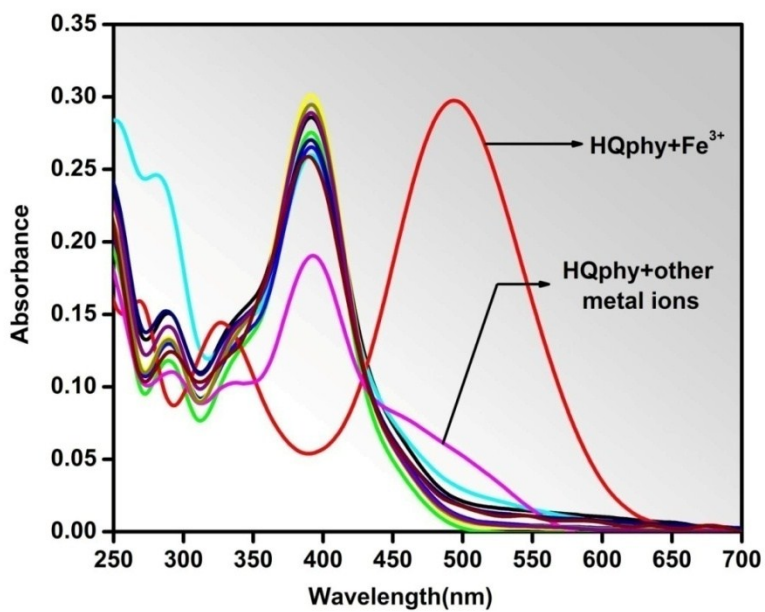


Fig. S9 UV-Vis absorption spectra of **HQphy** ($10\ \mu\text{M}$) upon addition of $10\ \mu\text{M}$ metal ions (perchlorate or chloride salts of Na^+ , K^+ , Ca^{2+} , Mg^{2+} , Hg^{2+} , Ni^{2+} , Fe^{3+} , Cu^{2+} , Co^{2+} , Cd^{2+} , Zn^{2+} , Fe^{2+} , Mn^{2+} , Cr^{3+} and Al^{3+}) in acetonitrile medium.

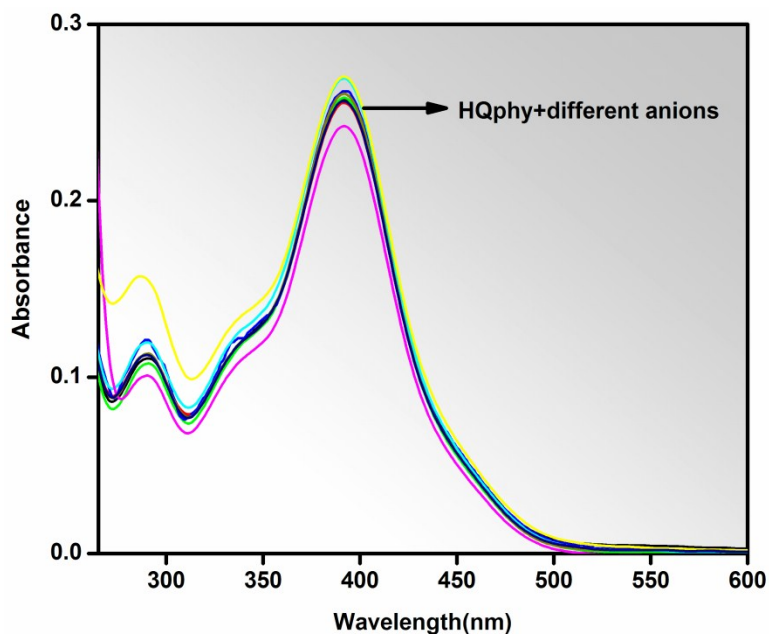


Fig. S10 UV-Vis absorption spectra of **HQphy** (10 μM) upon addition of 50 μM different anions (tetrabutyl ammonium salts of F^- , OAc^- , Cl^- , Br^- , I^- , HSO_4^- , NO_3^- , SCN^- , ClO_4^- and PF_6^-) in acetonitrile medium.

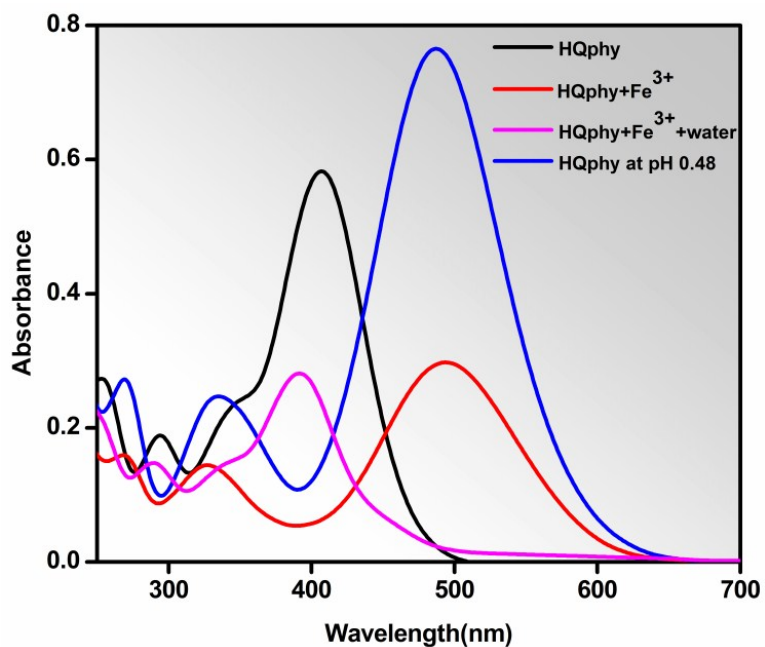


Fig. S11 UV-Vis absorption spectra of probe **HQphy** in presence of Fe^{3+} , water and at pH 0.48.

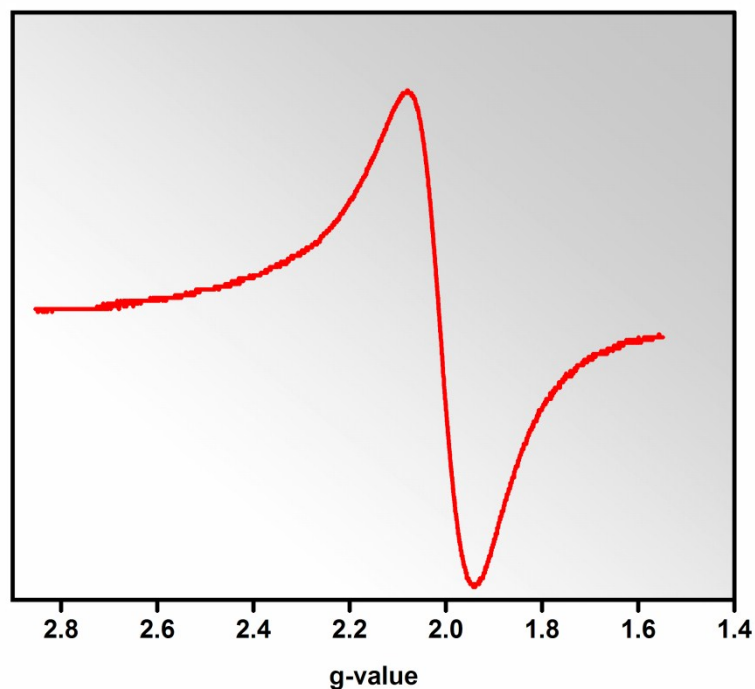


Fig. S12 X-band EPR spectra of solid $[\text{HQphy}][\text{FeCl}_4]\cdot\text{H}_2\text{O}$ (2) at room temperature (Frequency– 9.46494 GHz).

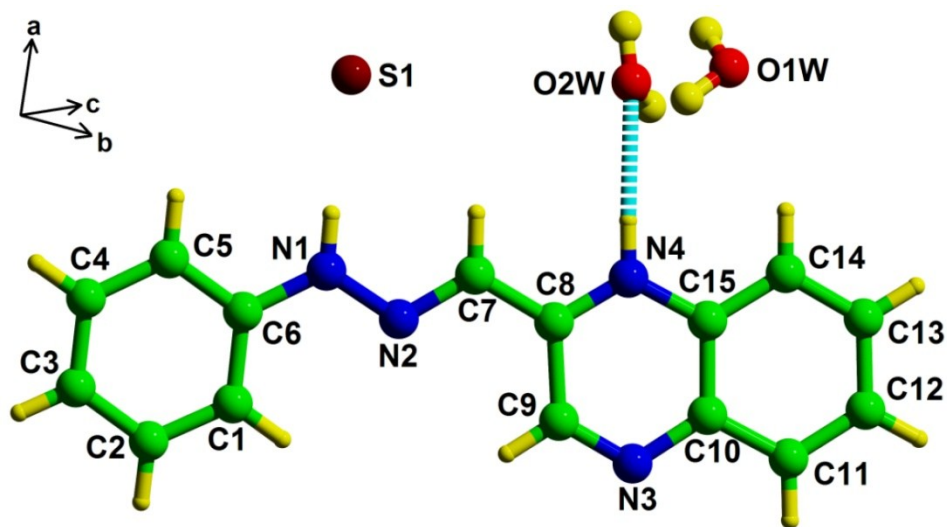


Fig. S13 Molecular structures of Compound 4 ($[\text{H}_2\text{Qphy}]_2\text{S}\cdot 4\text{H}_2\text{O}$) in ball and stick representation. Only H-bonds between protonated nitrogen (N4) and lattice water are shown as dotted turquoise bonds. The cation is disordered over a pseudo mirror plane through C7–H7, only the major component is shown. Color code: C = green; N = blue; O = red; S = maroon; H = yellow. (CCDC: 1847729)

Supramolecular structures of 1–4

The crystal packing of **1** is stabilised by H bonding between the amine hydrogen (HN1) of the phenyl hydrazine moiety and the quinoxaline nitrogen (N4) with an $N1\cdots N4$ ($1/2+x, 3/2-y, -z$) distance of 3.063(3) Å. Details of all hydrogen bonds are given in Table S4, ESI†. This hydrogen bonded entity is intercalated over each other by π – π stacking interaction between quinoxaline (X) and phenyl ring (Y), leading to the formation of infinite 1–D tape along crystallographic axis *a* (Fig. S14, ESI†).

In **2**, the adjacent molecules along *b* axis are connected by the $C_{\text{aromatic}}\text{--}H\cdots Cl$ and $N1\cdots Cl3$ (3.418(4) Å) interactions to form a tape comprised of protonated ligand and tetrahedral $FeCl_4^-$ moiety. These 1–D tapes form donor hydrogen bonds to the water molecule ($N4\cdots O1W$ 2.739(5) Å) which also forms a donor hydrogen bond to the $FeCl_4^-$ ion ($O1W\cdots Cl4$ 3.661(4) Å). The tapes are propagated along the *c* axis by hydrogen bonds from O1W to N3 ($x, 2-y, 1/2+z$) at 2.846(5) Å. The phenyl hydrazine moiety forms bifurcated π – π stacking with the two rings (both X and Z) of quinoxaline moiety. This van der Waals interaction stacks previously described 2–D layers over one another along *a* axis to form 3–D architecture (Fig. S15, ESI†).

In **3**, one of the quinoxaline nitrogens (N4) is protonated and hydrogen bonded to solvent water molecule ($N4\cdots O1W$ 2.685(3) Å). Strong hydrogen bonding is also observed between O1W and two perchlorate counter anions $O1W\cdots O4$ ($x, 1/2-y, 1/2+z$) and $O1W\cdots O2$ ($-x, 1/2+y, 1/2-z$) at 2.808(4) and 2.828(4) Å respectively. A closer look at the extended structure reveals a chair-like octameric self assembled $[(H_2O)_2(ClO_4)_2]^{2-}$ anion water cluster that generates a tilted helical chain of $[(H_2O)_2(ClO_4)_2]^{2-}$ cluster encapsulated in the 1–D supramolecular structure of **3**. Neighboring $[(H_2O)_2(ClO_4)_2]^{2-}$ units are connected through H–bonding between N1 and O2 ($-x, 1/2+y, 1/2-z$) and O1 ($x, 3/2-y, 1/2+z$) at 3.177(4), 3.060(4) Å respectively and π – π stacking between quinoxaline (X) and phenyl (Y) rings to form 1–D hydrophilic channel along *b* axis. This encapsulated water–perchlorate tapes are stitched to one another along *c* axis by $C_{\text{aromatic}}\text{--}H\cdots N3$ interactions to form a 2–D layer. This 2–D layer is converted to 3–D supramolecular architecture through $C_{\text{aromatic}}\text{--}H13/H14\cdots O3$ interactions along the *a* axis (Fig. S16, ESI†).

In **4**, two protonated ligands are hydrogen bonded through N1 along *a* axis to sulfur atom which is positioned on a two-fold axis with an N1...S1 distance of 3.169(3) Å. The central S²⁻ forms four coordinate hydrogen bond, in which the opposite positions are homoleptic. Orthogonal to the N-H...S interaction, the lattice water molecule (O1W and O2W) are extensively H-bonded to form a symmetry generated hexameric water tape of T6 (2) pattern as described by Infantes *et al.*¹ All two water molecules present in the lattice are mutually involved in hydrogen bonding interactions such that in a single water hexamer four symmetry generated O2W and two symmetry generated O1W are present thus having C4-symmetry. The O...O distance ranges from 2.748(4)–2886(3) Å. Thus in simple view, inbetween this coplanar infinite hexameric water channel S²⁻ are hydrogen bonded to form 2-D hybrid sulfide-water cluster of monomeric [S(H₂O)₆]²⁻ unit. Above and below this sheet hydrophobic cationic ligand is dimerised by hydrogen bonding via C-H...N interaction. The aromatic π rings (X and Z) undergo intermolecular π-π stacking interactions to stabilise the overall layered supramolecular structure (Fig. S17, ESI†). Thus overall a infinite 3-D supramolecular architecture is formed by alternate repeatation of hydrophilic sulfide-water sheet and hydrophobic protonated ligand. A comparative result discussed above on different π-π stacking observed on **1–4** is summarised in Table S3, ESI†.

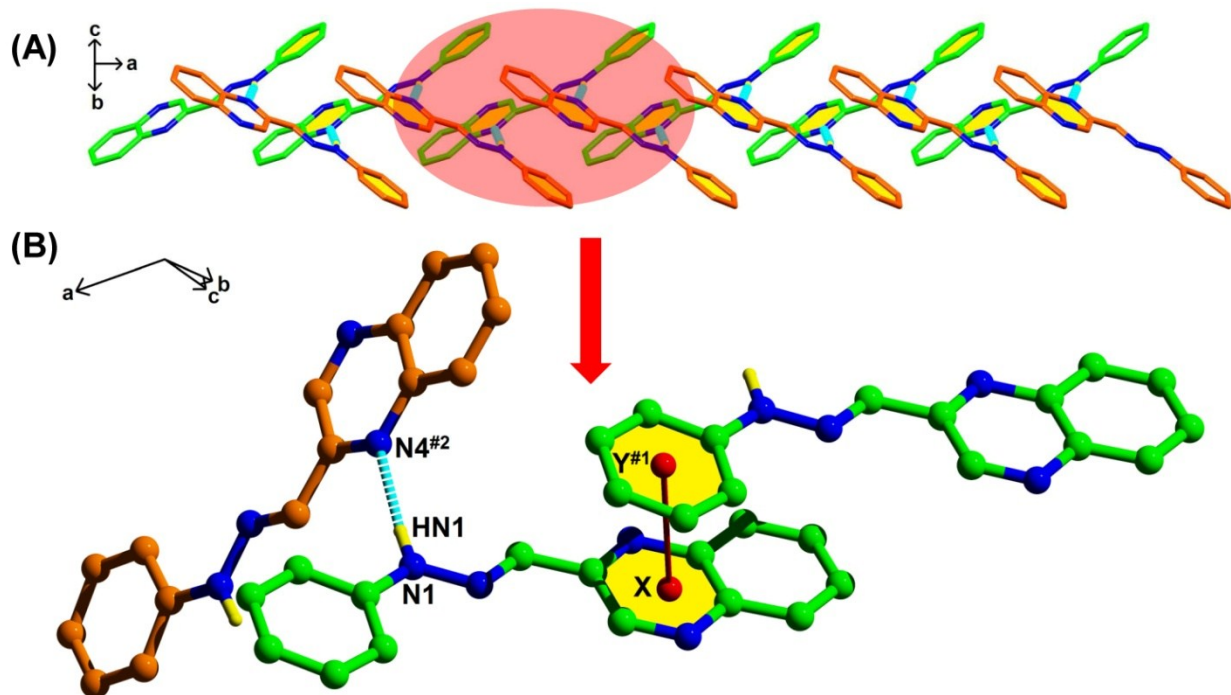


Fig. S14 (HQphy) (A) Infinite 1-D chain mediated by N-H \cdots N hydrogen bonding interactions and π - π interactions between parallel quinoxaline and phenyl moieties (two opposite intercalated nearly parallel tapes are shown in green and orange colors). (B) Enlarged view of π - π and N-H \cdots N hydrogen bonding interactions with partial atom numbering. The centroid X and Y are formed by atom groups C8 C9 N3 C10 C15 N4 and C1-C6 inclusive respectively. The centroid-centroid distance is 3.7032(14) Å. Turquoise bond represents the H-bond. Symmetry elements #1 (-1+x, +y, +z); #2 ($\frac{1}{2}$ +x, $\frac{3}{2}$ -y, -z).

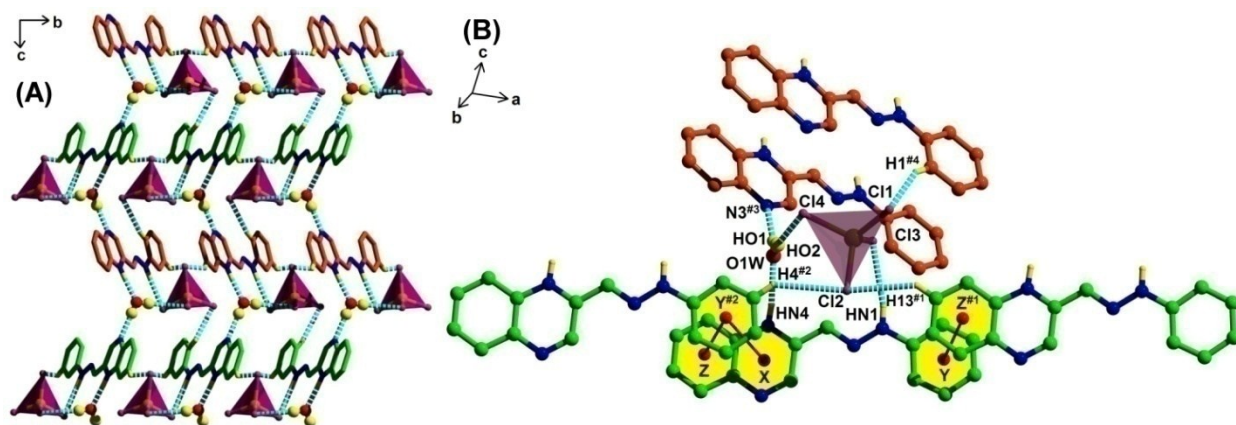


Fig. S15 ($[\text{H}_2\text{Qphy}][\text{FeCl}_4]\cdot\text{H}_2\text{O}$) (A) 3–D supramolecular association of protonated ligand with lattice water and tetrahedral FeCl_4^- ion (shown in polyhedra) (B) Local environment around tetrahedral FeCl_4^- ion stabilized by aromatic $\text{C-H}\cdots\text{Cl}$, $\text{N-H}\cdots\text{Cl}$, $\text{N-H}\cdots\text{O}$, $\text{O-H}\cdots\text{N}$ interactions and bifurcated π – π stacking between phenyl group and quinoxaline moiety. The three centroids X, Y, Z, are formed from rings containing atoms C8 C9 N3 C10 C15 N4, C1–C6 inclusive, C10–C15 inclusive respectively. Symmetry transformations are #1 ($1+x, -1+y, z$); #2 ($-1+x, y, z$); #3 ($x, 2-y, \frac{1}{2}+z$); #4 ($x, 1-y, \frac{1}{2}+z$). The marked centroid–centroid distances are 3.689(2) Å [$\text{X-Y}\#2$], 3.765(3) Å [$\text{Y}\#2\text{-Z}$], 3.869(3) Å [$\text{Y-Z}\#1$]. H–bonds are shown as dotted turquoise bonds.

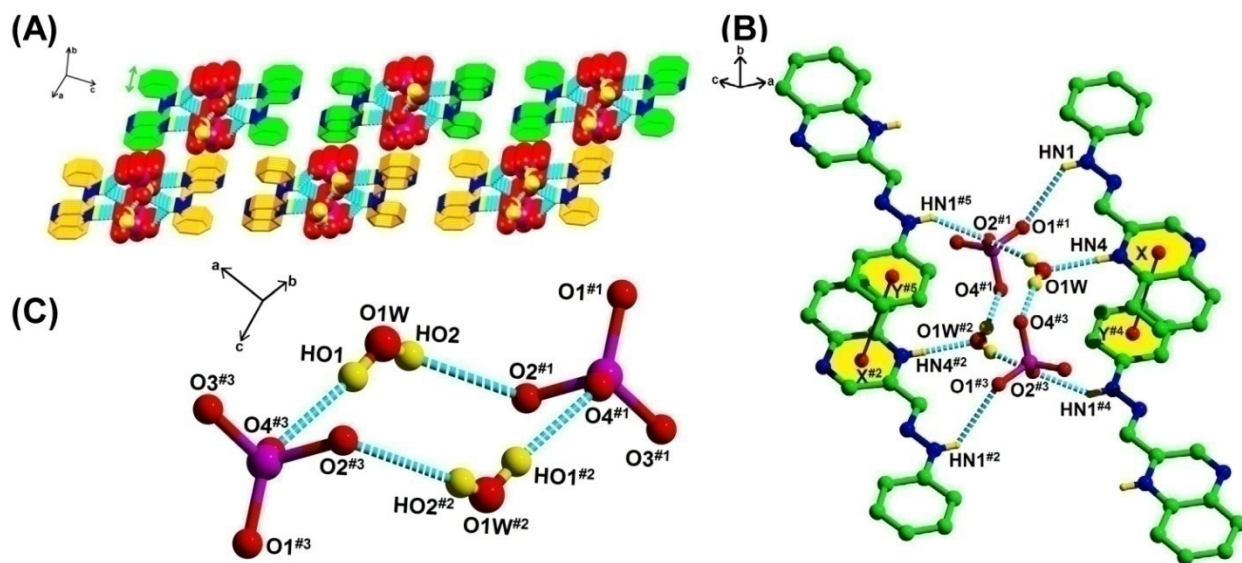


Fig. S16 ($[\text{H}_2\text{Qphy}]\text{ClO}_4 \cdot \text{H}_2\text{O}$) (A) Each of the octameric water-perchlorate clusters encapsulated by two ligand is stacked over one another through π - π stacking along the *b* axis. Along the *c* axis, this octameric entity interacts with another through C-H \cdots N interactions to form 2-D sheet. Each of the 2-D sheets are stitched over one another through Cl-O \cdots π interaction to form 3-D supramolecular interaction. (B) Enlarged view of water-perchlorate association via hydrogen bonding and π - π stacking. The centroids X, Y are formed from rings containing atoms C8 C9 N3 C10 C15 N4, and C1-C6 inclusive. The marked centroid-centroid distance is 3.618(2) Å. (C) Chair-like octameric association of $[(\text{H}_2\text{O})_2(\text{ClO}_4)_2]^{2-}$ anion water cluster. H-bonds are shown as dotted turquoise bonds. Symmetry code for the equivalent atoms, #1 ($-x, \frac{1}{2}+y, \frac{1}{2}-z$); #2 ($-x, 1-y, 1-z$); #3 ($+x, \frac{1}{2}-y, \frac{1}{2}+z$); #4 ($x, -1+y, z$); #5 ($-x, 2-y, 1-z$).

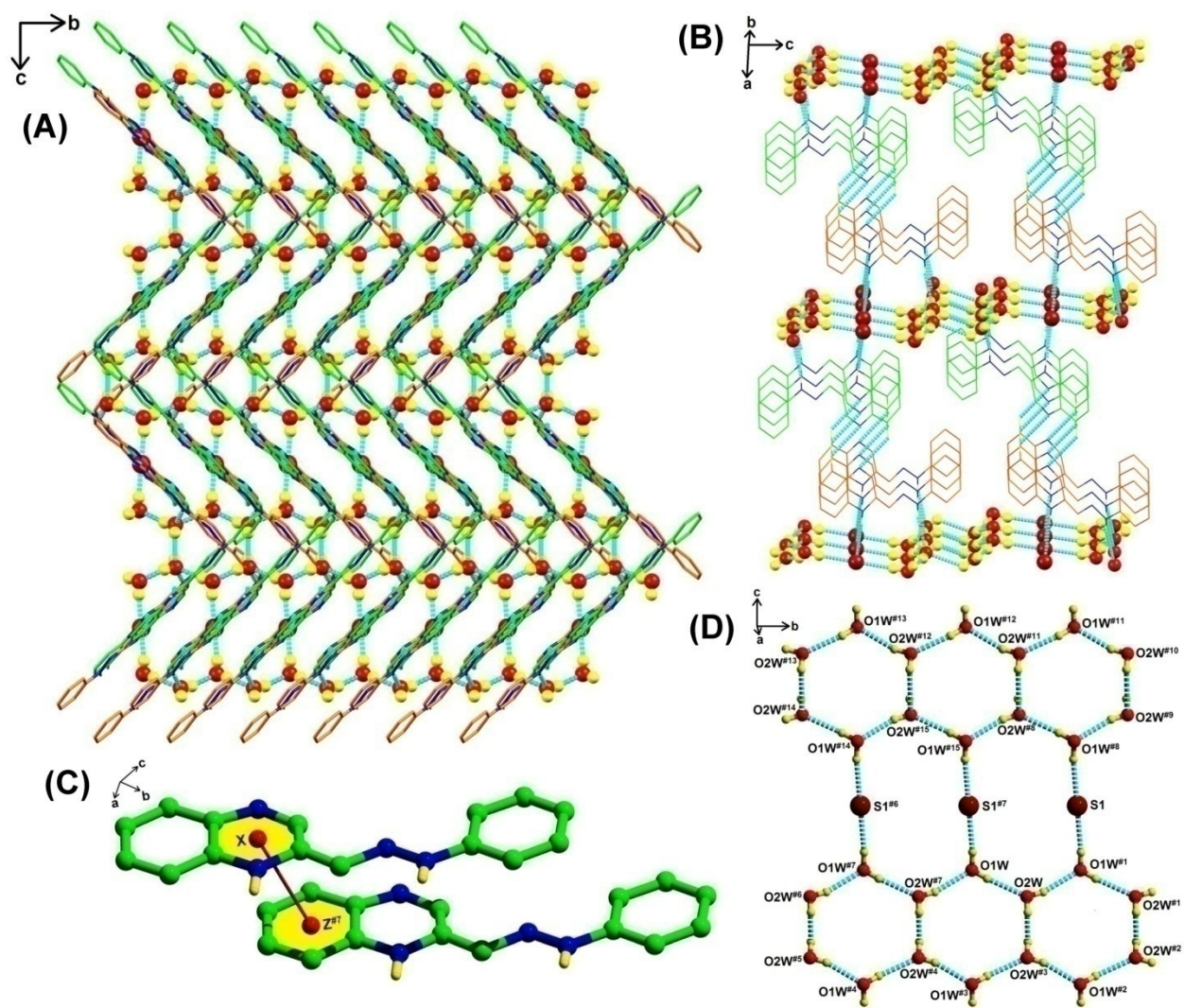


Fig. S17 ($[\text{H}_2\text{Qphy}]_2\text{S}\cdot 4\text{H}_2\text{O}$) (A) Infinite 3-D sheet like structure formed by various hydrogen bonding interactions $\text{N}-\text{H}\cdots\text{O}$, $\text{N}-\text{H}\cdots\text{S}$, $\text{O}-\text{H}\cdots\text{O}$, $\text{O}-\text{H}\cdots\text{S}$ (details in Table S6) and $\pi-\pi$ stacking seen through a axis. (B) Encapsulation of hydrophobic $\pi-\pi$ interaction mediated by cationic H_2Qphy within the hydrogen bonded 2-D layer of $[\text{S}(\text{H}_2\text{O})_6]^{2-}$. (C) Enlarged view of $\pi-\pi$ interaction with the centroids X and Z are formed by atom groups N1 C6 C1 N3X C9X C2X and C1-C6 inclusive respectively. The centroid-centroid distance is $3.530(3)$ Å. (D) Enlarged view of hydrogen bonded lattice water molecule to form 1-D water chain, which forms head-on hydrogen bonding via sulfide ion to another 1-D chain to form 2-D sulfide-water cluster. H-bonds are shown as dotted turquoise bonds. The symmetry elements #1 (+x, -1+y, +z); #2 (1-x, -1+y, 3/2-z); #3 (1-x, +y, 3/2-z); #4 (1-x, 1+y, 3/2-z); #5 (1-x, 2+y, 3/2-z); #6 (+x, 2+y, +z);

#7 (+x, 1+y, +z); #8 (1-x, 1-y, 1-z); #9 (1-x, -y, 1-z); #10 (+x, -y, -1/2+z); #11 (+x, 1-y, -1/2+z); #12 (+x, 2-y, -1/2+z); #13 (+x, 3-y, -1/2+z); #14 (1-x, 3-y, 1-z); #15 (1-x, 2-y, 1-z).

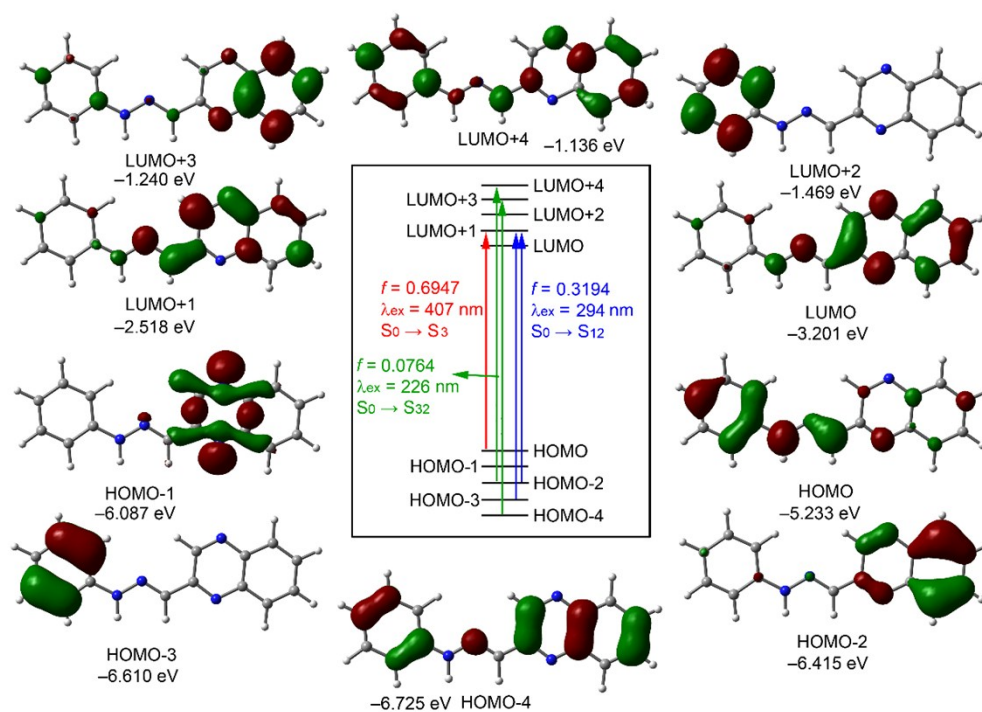


Fig. S18 Frontier molecular orbitals involved in three observable UV–Vis absorption bands of the probe.

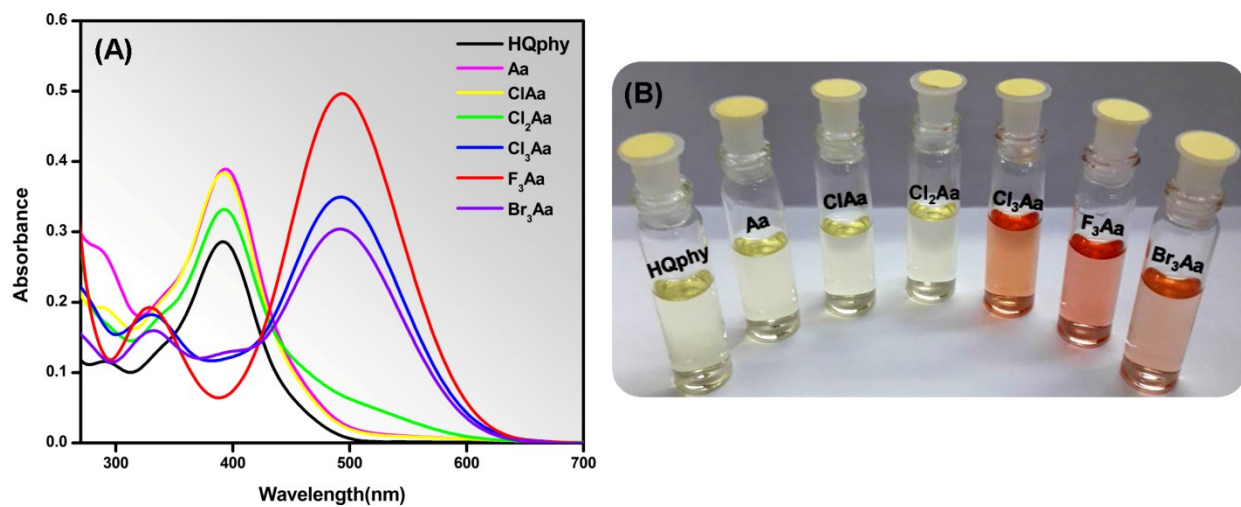
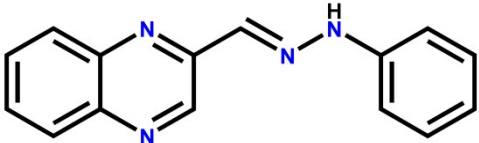
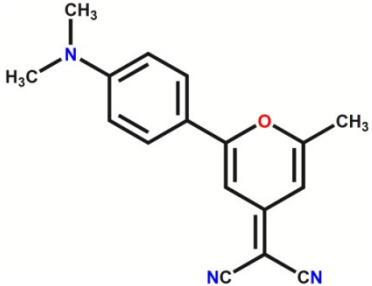
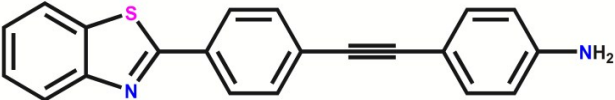
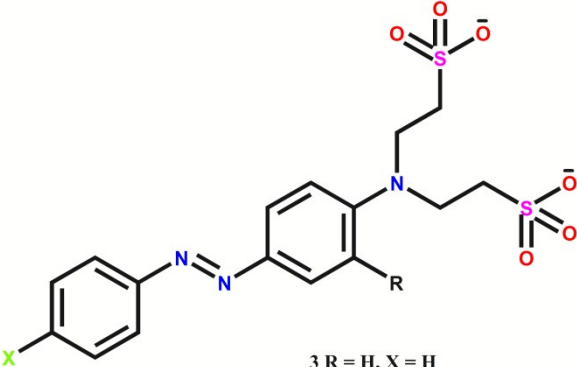
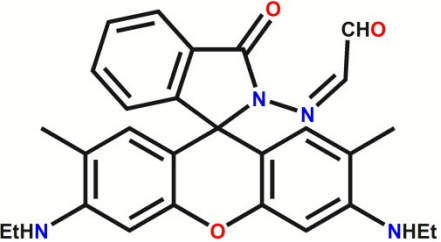


Fig. S19 (A) UV-Vis absorption spectra and (B) Visual color change of **HQphy** (10 μM) from yellow to red upon addition of 0.1 mM of different acetic acids (where, Aa = acetic acid).

Table S1 Strongly acidic pH sensing probes found in literature.

Entry	Probe	pK _a		Reference
1		1.67	Solely Colorimetric (391 nm to 492 nm)	this work
2		1.17	Both Colorimetric (440 nm to 369 nm) and Fluorometric	<i>Spectrochim. Acta Part A</i> , 2014, 122 , 304–308
3		1.34	Solely Fluorometric	<i>RSC Adv.</i> , 2013, 3 , 4872–4875
4	 <p>3 R = H, X = H 4 R = H, X = NO₂ 5 R = OCH₃, X = NO₂</p>	3: 2.15 4: 2.07 5: 2.58	Solely Colorimetric (3: 425 nm to 529 nm; 4: 481 nm to 542 nm; 5: 436 nm to 515 nm)	<i>Tetrahedron. Lett.</i> , 2014, 55 , 4559–4563
5		2.32	Solely Fluorometric	<i>Dyes Pigm.</i> , 2012, 95 , 112–115

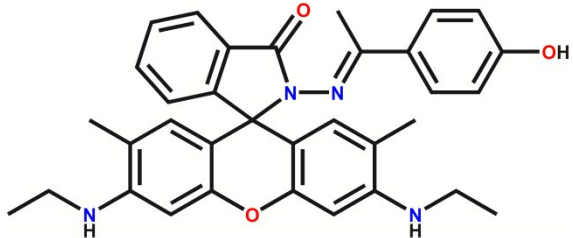
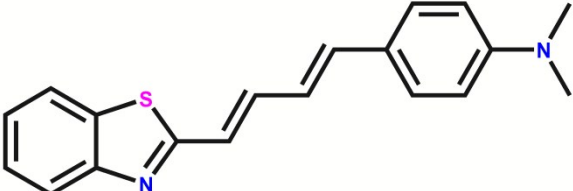
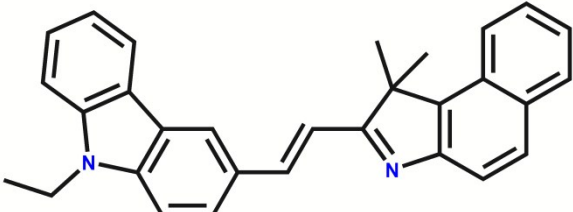
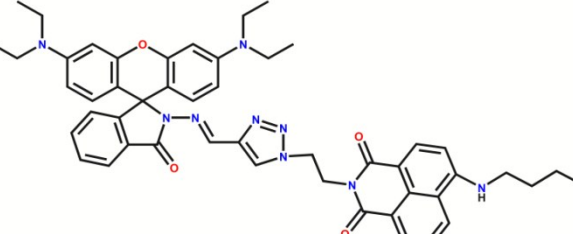
6		2.34	Both Colorimetric and Fluorometric	<i>Sens. Actuators B</i> , 2014, 194 , 498–502
7		2.34	Solely Fluorometric	<i>Sens. Actuators B</i> , 2016, 233 , 566–573
8		2.44	Both Colorimetric (400 nm to 505 nm) and Fluorometric	<i>Sens. Actuators B</i> , 2015, 221 , 1069–1076
9		2.79	Both Colorimetric and Fluorometric	<i>Dyes Pigm.</i> , 2013, 99 , 620–626

Table S2 Crystal Data and refinement details for complexes**1–4**

	1	2	3	4
CCDC No	1847716	1847717	1847723	1847729
Chem. Formula	C ₁₅ H ₁₂ N ₄	C ₁₅ H ₁₅ Cl ₄ FeN ₄ O	C ₁₅ H ₁₅ ClN ₄ O ₅	C ₃₀ H ₃₄ N ₈ O ₄ S
Formula weight	248.29	464.96	366.76	602.71
Crystallcolor, habit	orange/block	blue/block	green/block	blue/needle
Temp (K)	296(2)	295(2)	296(2)	297(2)
$\lambda^a/\text{\AA}$	0.71073	0.71073	0.71073	0.71073
Crystal system	orthorhombic	Monoclinic	Monoclinic	Monoclinic
Space group	<i>Pbca</i>	<i>Pc</i>	<i>P2₁/c</i>	<i>C2/c</i>
Unit cell dimensions				
<i>a</i> (Å)	7.356(2)	8.8038(3)	8.9676(12)	28.2924(16)
<i>b</i> (Å)	15.611(5)	7.6345(3)	8.2574(11)	4.8996(3)
<i>c</i> (Å)	21.490(7)	15.3532(6)	22.319(3)	22.2400(13)
β (deg)	90	96.2430(10)	94.520(4)	91.683(5)
Volume (Å ³), Z	2467.8(13),8	1025.81(7),2	1647.6(4),4	3081.6(3),8
Density (mg m ⁻³)	1.337	1.505	1.479	1.299
AbsorptionCoeff(mm ⁻¹)	0.084	1.266	0.267	0.154
F(000)	1040.0	470.0	760.0	1272.0
Crystal size (mm)	0.28×0.22×0.16	0.16×0.12×0.08	0.22×0.18×0.16	0.19×0.17×0.16
θ range (deg)	1.90–25.89	2.67–26.38	1.83–25.50	2.36–26.38
Limiting indices	-9≤ <i>h</i> ≤8 -19≤ <i>k</i> ≤18 -25≤ <i>l</i> ≤26	-10≤ <i>h</i> ≤11 -9≤ <i>k</i> ≤9 -19≤ <i>l</i> ≤19	-10≤ <i>h</i> ≤10 -10≤ <i>k</i> ≤9 -27≤ <i>l</i> ≤27	-34≤ <i>h</i> ≤34 -6≤ <i>k</i> ≤6 -27≤ <i>l</i> ≤26
Reflections collected	25790	12350	18334	21129
Unique reflections [<i>R</i> _{int}]	2370(0.070)	4077(0.042)	3043(0.034)	3132(0.049)
Completeness to θ	99.2%(25.89)	99.5%(25.24)	99.7%(25.50)	99.7%(25.24)
Data/restraints/parameters	2370/0/ 176	4077/7/240	3043 /5/238	3131/6/227
GOOF on F ²	0.941	0.971	1.043	1.047
R1 ^a , wR2 ^b values [<i>I</i> > 2 σ (<i>I</i>)]	0.0479, 0.1331	0.0317, 0.0789	0.05209, 0.1515 ^c	0.0701, 0.1992
R1 ^a ,wR2 ^b values (all data)	0.0858 ^b , 0.1596	0.0362, 0.0789	0.0695, 0.1677 ^c	0.1225, 0.2213
Maximum, minimumresidual peaks (e Å ⁻³)	0.170, -0.186	0.342, -0.298	0.422, -0.246	0.354, -0.254

^aGraphitemonochromator ^b $R_1 = \Sigma(|F_o| - |F_c|)/\Sigma|F_o|$. ^c $wR_2 = \{\Sigma[w(|F_o|^2 - |F_c|^2)^2]/\Sigma[w(|F_o|^2)^2]\}^{1/2}$

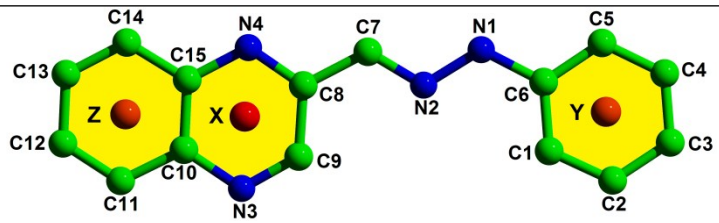
Table S3 Some important comparable metric parameters (distances, Å, angles (°)) in **HQphy**, **[H₂Qphy][FeCl₄]·H₂O**, **[H₂Qphy]ClO₄·H₂O** and **[H₂Qphy]₂S·4H₂O**.

Bond	HQphy	[H₂Qphy][FeCl₄]·H₂O	[H₂Qphy]ClO₄·H₂O	[H₂Qphy]₂S·4H₂O
N1–N2	1.330(2)	1.313(5)	1.309(3)	1.329(3)
C7–N2	1.275(2)	1.302(6)	1.296(4)	1.324(4)
C6–N1	1.373(2)	1.405(5)	1.396(3)	1.397(4)
C7–C8	1.432(2)	1.420(5)	1.412(4)	1.407(4)
C8–N4	1.309(2)	1.331(5)	1.331(3)	1.317(3)
C15–N4	1.362(2)	1.368(5)	1.362(4)	1.372(3)
Bond Angle				
N2–N1–C6	121.3(2)	122.3(3)	121.5(2)	121.3(3)
N1–N2–C7	117.3(2)	116.4(3)	117.7(2)	116.9(3)
N2–C7–C8	121.1(2)	118.9(4)	117.8(3)	119.0(3)
N1–C6–C1	121.7(2)	121.7(4)	121.0(3)	120.9(3)
N4–C8–C7	117.4(2)	119.4(4)	118.8(3)	118.9(2)

Table S4 Hydrogen bonds parameters in complex 1–4, (distances, Å, angles, (°)).

Donor–H···Acceptor	D–H	H···A	D···A	D–H···A	Symmetry elements
HQphy (1)					
N1–HN1···N4	0.85(2)	2.22(2)	3.063(3)	175(2)	$\frac{1}{2}+x, 3/2-y, -z$
[H₂Qphy][FeCl₄]·H₂O (2)					
N4–HN4···O1W	0.84(3)	1.90(3)	2.739(5)	172(5)	
N1–HN1···Cl3	0.87(3)	2.56(3)	3.418(4)	168(5)	
O1W–HO1···N3	0.85(3)	2.00(3)	2.846(5)	174(5)	$x, 2-y, \frac{1}{2}+z$
O1W–HO2···Cl4	0.85(2)	2.82(3)	3.661(4)	169(5)	
[H₂Qphy]ClO₄·H₂O (3)					
N4–HN4···O1W	0.84(2)	1.85(2)	2.685(3)	177(4)	
N1–HN1···O1	0.84(2)	2.55(3)	3.177(4)	132(3)	$-x, \frac{1}{2}+y, \frac{1}{2}-z$
N1–HN1···O2	0.84(2)	2.36(3)	3.060(4)	142(3)	$x, 3/2-y, z+\frac{1}{2}$
O1W–HO1···O4	0.83(2)	1.99(2)	2.808(4)	171(4)	$x, \frac{1}{2}-y, z+\frac{1}{2}$
O1W–HO2···O2	0.81(2)	2.06(2)	2.828(4)	157(4)	$-x, \frac{1}{2}+y, \frac{1}{2}-z$
[H₂Qphy]₂S·4H₂O (4)					
N4–HN4···O2W	0.77(3)	2.17(3)	2.920(3)	168(3)	
N1–HN1···S1	0.80(3)	2.38(3)	3.169(3)	169(3)	
O1W–HO11···O2W	0.88(2)	1.97(3)	2.808(4)	158(5)	
O1W–HO12···S1	0.88(2)	2.22(2)	3.100(3)	172(5)	$x, 1+y, z$
O2W–HO22···O2W	0.79(2)	2.35(1)	2.886(5)	126(1)	$1-x, y, 3/2-z$
O2W–HO21···O1W	0.79(2)	1.98(2)	2.748(4)	165(5)	$x, -1+y, z$

Table S5 Various π - π stacking interactions observed in complexes 1–4.



Complexes	Cg rings	Cg–Cg distance (Å)	Slippage(Å)
HQphy (1)	X–Y	3.703(1)	0.739
	X–Y	3.689(2)	1.555
[H ₂ Qphy][FeCl ₄]·H ₂ O (2)	Y–Z	3.869(3)	1.827
	Y–Z	3.766(3)	1.731
[H ₂ Qphy]ClO ₄ ·H ₂ O (3)	X–Y	3.618(2)	1.090
[H ₂ Qphy] ₂ S·4H ₂ O (4)	X–Z	3.530(3)	1.269

Table S6 Selected parameters for the vertical excitation (UV–Vis absorptions) of **HQphy**, electronic excitation energies (eV) and oscillator strengths (f), configurations of the low-lying excited states of **HQphy**; calculation of the S_0 – S_n energy gaps based on optimized ground-state geometries (UV–Vis absorption, acetonitrile used as solvent). For each electronic transition, only those contributions higher than 20% are given.

Process	Electronic transitions	Composition	Excitation energy (λ)	Oscillator strength (f)	λ_{exp} (nm)
Absorption	$S_0 \rightarrow S_3$	HOMO \rightarrow LUMO+1 (86%)	3.0415 eV (407 nm)	0.6947	391
Absorption	$S_0 \rightarrow S_{12}$	HOMO–3 \rightarrow LUMO+1 (38%) HOMO–2 \rightarrow LUMO+1 (22%)	4.2069 eV (294 nm)	0.3194	291
Absorption	$S_0 \rightarrow S_{32}$	HOMO–4 \rightarrow LUMO+3(54%) HOMO–2 \rightarrow LUMO+4(36%)	5.4840 eV (226 nm)	0.0764	228

Table S7 Selected parameters for the vertical excitation (UV–Vis absorptions) of protonated compound (**H₂Qphy⁺**), electronic excitation energy (eV) and oscillator strength (*f*), configurations of the lowest–lying excited state; calculation of the S₀–S_n energy gaps based on optimized ground–state geometries (UV–Vis absorption, in water solvent).

Process	Electronic transitions	Composition	Excitation energy (λ)	Oscillator strength (<i>f</i>)	λ_{exp} (nm)
Absorption	S ₀ → S ₁	HOMO → LUMO (100%)	3.0415 eV (483 nm)	1.0794	492

References

1. L. Infantes and S. Motherwell, *CrystEngComm*, 2002, **4**, 454–461.